AIP | Applied Physics Letters

Effective attenuation length for lanthanum lutetium oxide between 7 and 13 keV

A. Nichau, J. Rubio-Zuazo, M. Schnee, G. R. Castro, J. Schubert et al.

Citation: Appl. Phys. Lett. **102**, 031607 (2013); doi: 10.1063/1.4789524
View online: http://dx.doi.org/10.1063/1.4789524
View Table of Contents: http://apl.aip.org/resource/1/APPLAB/v102/i3
Published by the American Institute of Physics.

Effective attenuation length for lanthanum lutetium oxide between 7 and 13 keV

A. Nichau,[1] J. Rubio-Zuazo,[2] M. Schnee,[1] G. R. Castro,[2] J. Schubert,[1,a)] and S. Mantl[1]
[1]*Peter Grünberg Institute 9, Forschungszentrum Jülich and JARA-FIT, 52425 Jülich, Germany*
[2]*Spanish CRG BM25 Beamline–SpLine, European Synchrotron Radiation Facility (ESRF), Rue Jules Horowitz BP 220, F-38043 Grenoble Cedex 09, France*

(Received 4 December 2012; accepted 14 January 2013; published online 25 January 2013)

To obtain quantitative depth information from hard X-ray photoemission spectroscopy, the effective attenuation length (EAL) is required. In this paper, the EAL was determined for $LaLuO_3$ for electron kinetic energies between 7 and 13 keV. As a result, the EAL is in the range of 100–150 Å for the investigated photon energies. In addition, higher binding energy orbitals of La and Lu were measured and are discussed. $LaLuO_3$ is a promising high-k dielectric for future nano-scaled MOS devices. © *2013 American Institute of Physics*. [http://dx.doi.org/10.1063/1.4789524]

It has previously been shown that lanthanum lutetium oxide ($LaLuO_3$) is a promising higher-k dielectric. Its high relative permittivity of ~32 in the amorphous state in conjunction with low leakage current densities make $LaLuO_3$ a candidate for the integration into future CMOS technology nodes.[1–5] A vital question for the integration is a deep knowledge of interface and material properties under temperatures typical for CMOS processing. In general, lanthanides and their compounds are of increasing importance for today's and future electronic applications. A suitable method for the study of lanthanides and their (buried) interface chemistry (e.g., to silicon) is hard X-ray photoemission spectroscopy (HAXPES).

However, the study of interface chemistry and of buried materials requires a detailed depth information and knowledge of the oxide's orbitals. A typical measure for the information depth for photon emission in a solid is the effective attenuation length (EAL) of the material.[6] In our paper, results on the EAL determination for $LaLuO_3$ between 7 and 13 keV will be presented. Furthermore, first results for the measurement of photon emission from La and Lu orbitals will be presented, which might be of general interest.[7]

The material of interest $LaLuO_3$ was deposited by pulsed-laser deposition (PLD) on low-doped Si substrates from a stoichiometric target under ambient oxygen. Prior to deposition, the Si substrates were cleaned with a standard RCA clean, leaving a thin chemical oxide on the Si substrate (1 nm). Two samples were prepared: A thin film with 12.4 nm thickness (determined by X-ray reflectivity (XRR)) and a bulk layer of 124 nm. The mass density for the PLD grown films was ~8.62 g/cm^3 as also found for our molecular beam deposition samples.[8]

HAXPES measurements were carried out at the CRG Spanish beamline (SpLine) at the European Synchrotron Radiation Facility (ESRF), Grenoble. The kinetic energy of the incoming photons was chosen as 10, 12, and 14 keV. At 14 keV, no Si substrate signal could be recorded for the thick sample. Thus, bulk properties can be assumed for this film at the chosen photon energies. The spectra were measured by a high voltage cylindrical sector analyzer Focus CSA 300/15 (Ref. 9) and calibrated against the chemical shift of the Si 1s signal from Si substrate, visible for the thin sample (binding energy (BE) = 1839.2 eV[10]). The Gaussian peak width is given by the beam line optics and corresponds to 1.5 eV, 1.8 eV, and 2.1 eV for 10, 12, and 14 keV, respectively.

The intensities for bulk material and thin overlayer on Si were recorded together with the photon flux of the beamline. Subsequently, the measured spectra were normalized to the mean beamline current. Spectra obtained during ring injection were discarded. Due to the same transmission and photon cross section, bulk and overlayer spectra were not needed to be normalized any further. The effective attenuation length can then be determined[6] energy-dependent from the intensity ratio $I_{overlayer}/I_{bulk}$ of overlayer and bulk film as given by

$$EAL = \frac{t_{overlayer}}{\ln\left(1 - \left(\frac{I_{overlayer}}{I_{bulk}}\right)\right)\cos\theta}, \quad (1)$$

where $t_{overlayer}$ is the thickness of the thin overlayer and $\theta = 15°$ is the collection angle formed between the analyzer and the sample normal. Error analysis for the peak fits was done by Monte-Carlo simulation within the software CASAXPS 2.3.17. Deviations from a pure Poissonian noise distribution due to the 2d event counting system were thereby neglected. Error estimation for the EAL values was done by subsequent application of the Gaussian propagation law.

The lanthanide orbitals measured show strong plasmon features. They increase for the bulk material suggesting both surface and bulk plasmon contributions. The La 3d orbitals displayed in Fig. 1(a) possess strong satellites shifted by 4.5 eV with intensities of 70% of the main peaks. Similar structures were before observed for La_2O_3 by Teterin.[11,12] For higher photon energy (not shown here), satellites and peaks merge due to the broader energy distribution. La $3d_{5/2}$ and La $3d_{3/2}$ are separated by 16.8 eV, comparable to results found for La_2O_3 by Sunding.[13] Increasing plasmon contributions are visible if comparing bulk and overlayer samples. These loss structures as previously described by Crecelius *et al.*[14] increase for the bulk. There are low energy satellites present and bulk plasmon features around +13.8 eV away

a)Email: j.schubert@fz-juelich.de.

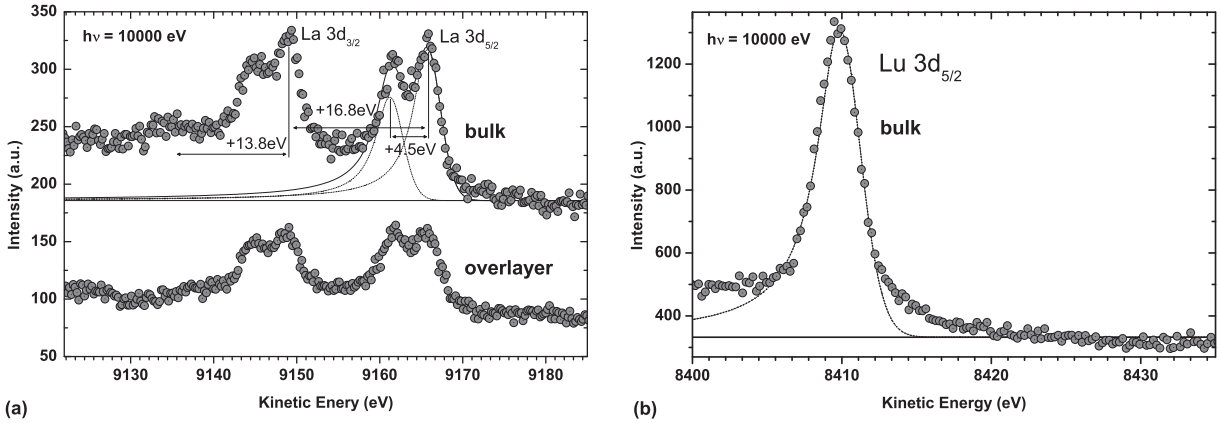

FIG. 1. (a) Bulk and overlayer intensity of La 3d in $LaLuO_3$. A strong satellite feature is present at higher binding energy (keV) accompanied with satellite loss at low binding energy. Plasmon loss is increased for the bulk sample. A Doniach-Sunjic profile convoluted with a Voigt profile was used for deconvolution. (b) Lu $3d_{5/2}$ shows much less loss compared to La. No satellite structure was observed due to the completed electron configuration. FWHM is 3.2 eV.

from La $3d_{3/2}$. These plasmon features most prominent for the bulk material lead to an increasing background signal between La $3d_{5/2}$ and La $3d_{3/2}$ exacerbating the background subtraction during peak fitting.

The best agreement of our EAL value with the theoretical predictions[15–17] of the TPP-2M formula were found if a Doniach-Sunjic (DS) profile was used for peak fitting (cf. Fig. 1) as suggested by Crecelius *et al*. A Shirley background type with a pure Voigt profile lead to random scatter in the EAL prediction most likely dependent on the loss structures as described previously. This was also the case if we used the Gaussian width determined for the beamline optics in combination with a Lorentzian width as tabulated.[18] In our calculations, we thereby ignored the loss structure by the choice of the DS fit. As the DS profile is only asymptotically vanishing, its use becomes problematic. To circumvent these limitations, a convolution of a Voigt-type and DS profile was employed. This profile type results in a much faster decay. Moreover, the deconvolution of bulk and overlayer intensity leads to comparable decays in our case, so that the error imposed by the profile is judged to be minor in comparison to the noise in HAXPES measurements. The deconvolution resulted in a main peak for La $3d_{5/2}$ at a BE of 834.4 eV.

Lu $3d_{5/2}$ is shown in Fig. 1(b) together with a DS-type fit. We attribute the absence of a satellite structure to the trivalent configuration Lu^{3+} ([Xe] $4f^{14}$) with fully occupied f-shell. Also less shake-down[14] background is observed. Here, a constant background signal at lower binding energy was chosen for background subtraction, thereby revealing the low energy loss structure. The employed constant background depends on the accumulated signal during measurements. Fluctuations in ring current or injections can thereby lead to artificial patterns or intensity drops. A thorough inspection of every single scan must be employed in advance.

A selection of peaks used for determination of the EAL is shown in Fig. 2. All structures show a common loss structure at lower binding energy[14] and have a skewed structure due to the plasmon loss. The loss structure observed is mainly due to bulk plasmon loss as seen when comparing measurements for bulk and overlayer (Fig. 2(b)). Thereby the determination of the correct peak area is strictly dependent on the loss structure and subject to error. The best results were achieved if the constant background could be determined precisely. Likewise we had to set the energy range accordingly wide to screen this background (10-20 eV before rise of the first energy loss). However, for very broad loss and peak structures as in Fig. 2(d), the setup of the appropriate energy window is difficult and also limited by scheduled beam time.

The resulting effective attenuation length is plotted in Fig. 3 and summarized in Table I together with the peak positions found. As mentioned, the error bars are based on an error calculation for the peak models based on a Monte-Carlo simulation of possible peak models. Errors between 9 and 40 Å were found. The EAL was fitted by a power law $EAL \sim 0.11\ E_{kin}^{0.77}$. This result is in close agreement with the theoretical prediction for the inelastic electron mean free path (IMFP) obtained by the TPP-2M formula (Tanuma, Powell, Penn[16,19]). The IMFP should exceed the EAL in the solid.[20] We attribute the complicated loss structures in La and Lu to cause a systematic deviation from IMFP.

The uncertainty in EAL determination was higher for O 1s due to the overlayer signal consisting both of SiO_2 from the substrate. Lu 3s could also be determined with higher uncertainty due to the broad loss structure at lower binding energy (max. ±58 Å). A possible solution for O 1s would be the growth of amorphous $LaLuO_3$ on an oxide-free substrate (i.e., not silicon). Further improvements are likely possible for the overlayer method,[6] if orbitals with a large cross section and less electron loss structures would be used. However, the second requirement seems to be more difficult for La than for Lu because of the observation of loss structures in every orbital.

Lanthanide oxides in general and the investigated $LaLuO_3$ have gained increasing attention for applications in nanoelectronics in the past years. For a successful integration into nanoelectronics, a detailed knowledge of the film properties under processing temperatures is important. HAXPES measurements allow the study of thin film stacks as used in CMOS gate stacks. This paper presented a determination of the effective attenuation length of $LaLuO_3$ required for quantitative, undestructive depth profiles in the thin films. Moreover, measurements for high binding energy La and Lu orbitals, rarely reported in the literature were shown. The determination of the effective attenuation length in lanthanide compounds is

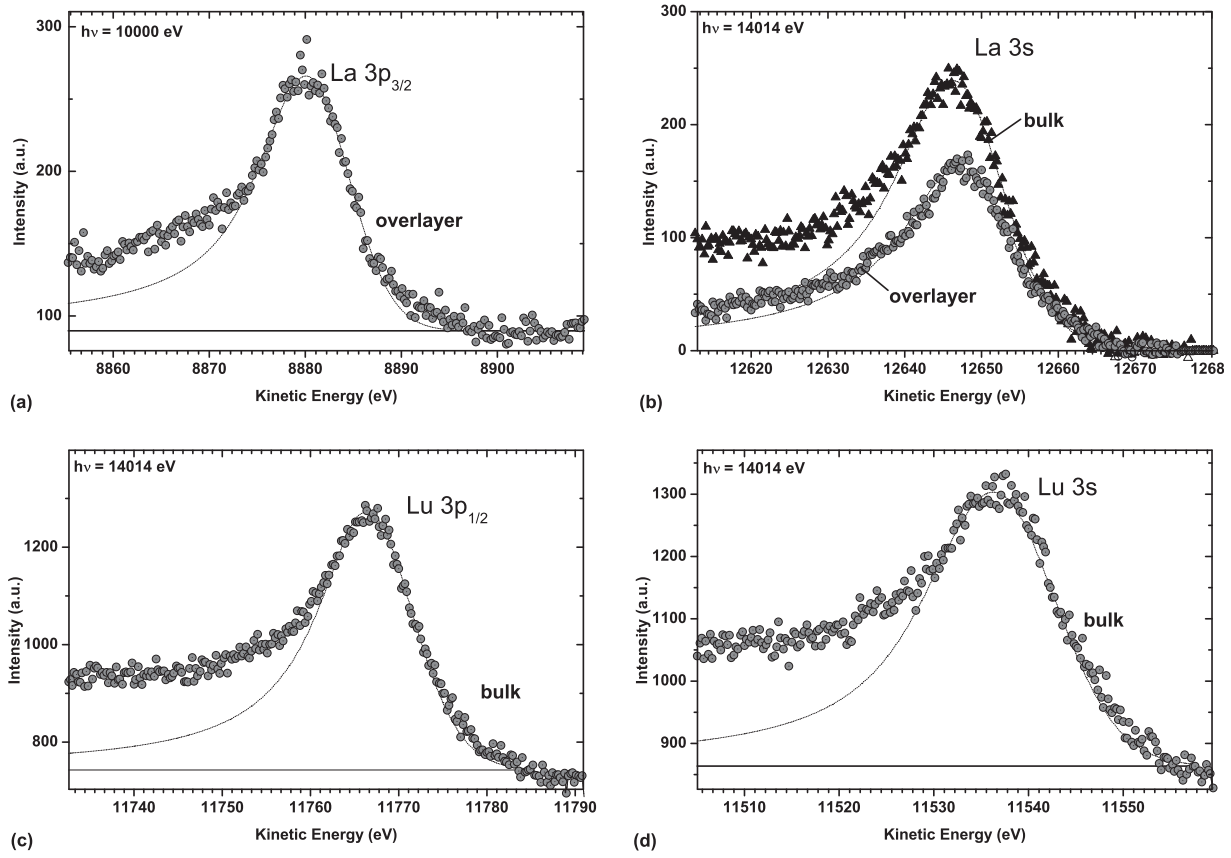

FIG. 2. Selection of oxide orbitals collected during EAL determination. (a) La $3p_{3/2}$ for thin material (PE = 10 keV). This orbital shows loss structures to lower and higher binding energy. FWHM is 10 eV for the Voigt profile of the fit. (b) La 3s comparing bulk and overlayer loss structure after constant background subtraction: Higher binding energy loss structures for bulk material are much more pronounced than for the overlayer and increasing with photon energy (14 keV). FWHM is 16.3 eV. (c) Lu $3p_{1/2}$ shows a similar structure as observed for La (FWHM = 12 eV). (d) Lu 3s is a broad peak with distinct loss structure at higher binding energy (PE = 10 keV, FWHM = 14 eV).

exacerbated by the present loss structures. However, the EAL as determined by the depth profile method is consistent with the theoretical predictions of Tanuma *et al.* The EAL in $LaLuO_3$ was determined to lie between ~100 Å and 150 Å for 7 to 13 keV. The obtained values are mainly subject to errors from the determination of the peak areas. The best agreement with the theoretical prediction was found for a Doniach-Sunjic profile[21] convoluted with a Voigt profile. A combination of Voigt profile and Shirley[22] background lead to erroneous and random scatter in the EAL values. The Voigt profile included more loss dependence on the Lorentzian width. Future studies

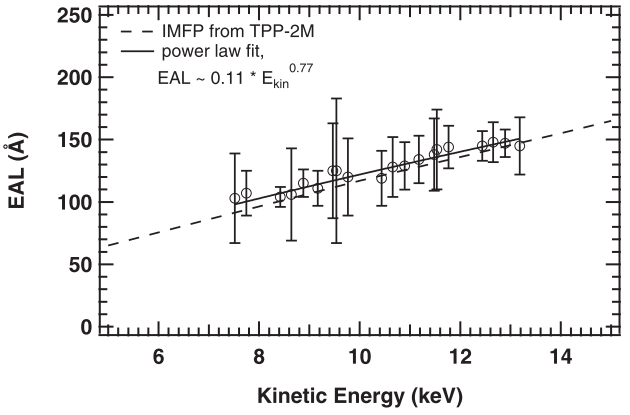

FIG. 3. Effective attenuation length for $LaLuO_3$ as determined by the depth profile method for 7 to 13 keV. The result is in agreement with the theoretical predictions of the TPP-2M model. Error bars are obtained by the Gaussian propagation law on the bases of peak fit and experimental errors (analyzer angle, XRR thickness). An error calculation based on min/max or standard deviation of the fitted values would clearly underestimate the errors due to deconvolution.

TABLE I. Summary of the peak positions and EAL values found by using the depth profile method.

Orbital		hν (eV)	E_{bind} (eV)	EAL (Å)	ΔEAL (Å)
Lu	3s	10 000	2494.9	103	36
Lu	$3p_{1/2}$	10 000	2265.6	107	19
Lu	$3d_{5/2}$	10 000	1590.3	104	9
La	3s	10 000	1371.3	106	37
La	$3p_{3/2}$	10 000	1128.4	115	11
La	$3d_{5/2}$	10 000	834.3	111	15
O	1s	10 000	530.3	125	38
Lu	3s	12 017		126	58
Lu	$3p_{1/2}$	12 017		120	31
Lu	$3d_{5/2}$	12 017		120	22
La	3s	12 017		129	24
La	$3p_{3/2}$	12 017		130	19
La	$3d_{5/2}$	12 017		135	19
O	1s	12 017		139	30
Lu	3s	14 017		143	32
Lu	$3p_{1/2}$	14 017		145	17
Lu	$3d_{5/2}$	14 017		146	13
La	3s	14 017		148	17
La	$3p_{3/2}$	14 017		147	12
La	$3d_{5/2}$	14 017		145	24

could clarify the origin of these loss structures to improve the deconvolution with Voigt profiles.

This work was partially supported by the project KZWEI which is funded in line with the technology funding for regional development (ERDF) of the European Union and by funds of the Free State of Saxony. Additional funding was received by the Nanosil network from the European Community (FP7 Grant No. 216171).

We would like to thank the SpLine staff for their valuable help in carrying out this research. Neal Fairley of CasaXPS Ltd., is acknowledged for providing all XPS and HAXPES import filters and his continued expert support.

[1]A. Nichau, E. Durgun Özben, M. Schnee, J. M. J. Lopes, A. Besmehn, M. Luysberg, L. Knoll, S. Habicht, V. Mussmann, R. Luptak, S. Lenk, J. Rubio-Zuazo, G. R. Castro, D. Buca, Q.-T. Zhao, J. Schubert, and S. Mantl, Solid-State Electron. **71**, 19–24 (2012).

[2]J. M. Lopes, E. Durgun Özben, M. Schnee, R. Luptak, A. Nichau, A. Tiedemann, W. Yu, Q.-T. Zhao, A. Besmehn, U. Breuer, M. Luysberg, S. Lenk, J. Schubert, and S. Mantl, ECS Trans. **35**, 461–479 (2011).

[3]E. Durgun Özben, J. M. J. Lopes, A. Nichau, M. Schnee, S. Lenk, A. Besmehn, K. K. Bourdelle, Q.-T. Zhao, J. Schubert, and S. Mantl, IEEE Electron Device Lett. **32**, 15–17 (2011).

[4]W. Yu, B. Zhang, Q.-T. Zhao, J.-M. Hartmann, D. Buca, A. Nichau, E. Durgun Özben, J. M. J. Lopes, J. Schubert, B. Ghyselen, and S. Mantl, in *Proceedings of 6th Workshop of the Thematic Network on Silicon-on-Insulator Technology (EUROSOI)* (2010), pp. 25–26.

[5]W. Yu, E. Durgun Özben, B. Zhang, A. Nichau, J. M. J. Lopes, R. Luptak, S. Lenk, J.-M. Hartmann, D. Buca, K. K. Bourdelle, J. Schubert, Q.-T. Zhao, and S. Mantl, in *2010 10th IEEE International Conference on Solid-State and Integrated Circuit Technology* (IEEE, 2010), pp. 875–878.

[6]J. Rubio-Zuazo, P. Ferrer, and G. R. Castro, J. Electron Spectrosc. Relat. Phenom. **180**, 27–33 (2010).

[7]P. Burroughs, A. Hamnett, A. F. Orchard, and G. Thornton, J. Chem. Soc., Dalton Trans. **17**, 1686–1698 (1976).

[8]J. M. J. Lopes, E. Durgun Özben, M. Roeckerath, U. Littmark, R. Luptak, S. Lenk, M. Luysberg, A. Besmehn, U. Breuer, J. Schubert, and S. Mantl, Microelectron. Eng. **86**, 1646–1649 (2009).

[9]J. Rubio-Zuazo, M. Escher, M. Merkel, and G. R. Castro, Rev. Sci. Instrum. **81**, 043304 (2010).

[10]*NIST X-ray Photoelectron Spectroscopy Database, Version 4.0* (National Institute of Standards and Technology, Gaithersburg, 2008).

[11]Y. A. Teterin and A. Y. Teterin, Russ. Chem. Rev. **71**, 347–381 (2002).

[12]Y. A. Teterin, A. Y. Teterin, A. M. Lebedev, and K. E. Ivanov, J. Electron Spectrosc. Relat. Phenom. **137–140**, 607–612 (2004).

[13]M. F. Sunding, K. Hadidi, S. Diplas, O. M. Løvvik, T. E. Norby, and A. E. Gunnæs, J. Electron Spectrosc. Relat. Phenom. **184**, 399–409 (2011).

[14]G. Crecelius, G. K. Wertheim, and D. N. E. Buchanan, Phys. Rev. B **18**, 6519–6524 (1978).

[15]S. Tanuma, C. J. Powell, and D. R. Penn, Surf. Interface Anal. **17**, 911–926 (1991).

[16]S. Tanuma, C. J. Powell, and D. R. Penn, Surf. Interface Anal. **21**, 165–176 (1994).

[17]S. Tanuma, C. J. Powell, and D. R. Penn, Surf. Interface Anal. **43**, 689–713 (2011).

[18]M. O. Krause and J. H. Oliver, J. Phys. Chem. Ref. Data **8**, 329 (1979).

[19]S. Tanuma, C. J. Powell, and D. R. Penn, Surf. Interface Anal. **20**, 77–89 (1993).

[20]D. Briggs and M. P. Seah, editors, *Practical Surface Analysis. 1. Auger and X-ray Photoelectron Spectroscopy*, Volume 1 (John Wiley & Sons, Hoboken, NJ, USA, 1990), p. 657.

[21]S. Doniach and M. Sunjic, J. Phys. C: Solid State Phys. **3**, 285–291 (1970).

[22]D. Shirley, Phys. Rev. B **5**, 4709–4714 (1972).